

Forecasting gamma radiation levels using digital image processing

Abou-Bakr M. Ramadan¹, Ahmed M. El-Garhy², Fathy Z. Amer², and Mazhar M. Hefnawi^{1*}

¹ Department of National Network for Monitoring Radioactivity, Atomic Energy Authority of Egypt, Cairo, Egypt

² Department of Electronics, Communications and Computers, Faculty of Engineering, Helwan University, Cairo, Egypt.

mmaazz_2222@yahoo.co.uk

Abstract: This work introduces a new way for data visualization. Its name is " Digital 'application name' Image". Normal digital image is created by digital camera or digital scanner but digital application name image is created by measurements of monitoring data. This work uses the data which is measured by some radiation monitoring stations and classifies it using fuzzy logic rules to create some digital radiation images. The main unique advantage of digital radiation image is that it expresses thousands of measurements in a very clear form through only one picture while the maximum number of measurements does not exceed 100 for other conventional visualization methods. This feature gives a facility to view one year of all recorded measurements in only one photo. This picture helps the user to observe the behavior of thousands of measurements in few minutes instead of spending few hours in reviewing hundreds of charts for the same measurements. This work also introduces a new way for forecasting Gamma radiation levels. This way uses image restoration technique to predict the gamma levels. Of course, this technique is used after creating digital radiation image. The quality for the output result from this model is at least accepted for forecasting and covering lost data. The main feature from this model is that it needs only one kind of data while other prediction models need at least three kinds of data. Therefore this model covers the common limitation in famous prediction models and saves money, time and effort.

[Abou-Bakr M. Ramadan, Ahmed M. El-Garhy, Fathy Z. Amer, and Mazhar M. Hefnawi. **Forecasting gamma radiation levels using digital image processing**. Life Science Journal 2012;9(1):701-710]. (ISSN: 1097-8135). <http://www.lifesciencesite.com>. 101

Keywords: Data Visualization; Digital Image Processing; Digital Radiation Image; Environmental Forecast.

1. Introduction:

This work describes a novel approach for encoding a set of continuous numerical observations in a form of a color image, where the coordinates of each pixel encode time of a specific observation and color represents magnitude of an observation. This work also uses this color image to generate a new approach for predicting future or missing observations from collected ones and compares this approach to artificial neural network and various deterministic classification algorithms. It is preferred to start with reviewing the basic definition of an image because it is a necessary part for explaining the definition of the digital measurements image.

An image may be defined^[1] as a two-dimensional function, $f(x,y)$, where x and y are spatial (plane) coordinates and the amplitude of f at any pair of coordinates (x,y) is called intensity of the image at that point. The term gray level is used often to refer to the intensity of the monochrome images. Color images are formed by a combination of individual 2-D images such as RGB color system, a color image consists of three (red, green, and blue) individual component images. So converting such an image to digital form requires that the coordinates, as well as the amplitude, be digitized. Digitizing the coordinate values is called sampling; digitizing the

amplitude values is called quantization. Thus when x,y and the amplitude values of f are all finite, discrete quantities. We call the image a digital image as shown in Fig. 1a for digital representation for monochrome image^[1] and Fig. 1b for digital representation of RGB color system image^[1].

2. Experimental

Digital measurements image like digital image has two-dimensional function, $f(x,y)$, but x and y are spatial (plane) coordinates indicate the date and time for each measurement. The amplitude of f at any pair of coordinates (x,y) is called intensity of the image at that point which is the value of the measurement as shown in Fig. 2a.

Construction of digital radiation image

Digital radiation image is a digital RGB color measurements image for radiation levels in ambient air. These measurements are measured by a radiation monitoring station. This station is in constant place and operating for 24 hours daily. It measures a radiation level in ambient air every 15 minutes^[2]. As shown in Fig. 2b the digital RGB color measurements image may be viewed as a "stack" of three gray-scale images that, when fed into red, green and blue inputs of a color monitor, produce a color image on the

screen. By convention, the three images forming an RGB color image are referred to as the red, green, and blue component images. The x and y coordinates for this image represent the date and time for each measurement. The color for each pixel in this image represents the measurement value.

Representing digital radiation image using different colors is better than representing it using 16 bit grayscale because it is easier and faster for human to watch and analyze the behavior of Gamma radiation levels in form of different colors than grayscale. The color image is a good choice for measurements of radiation levels because the nature behavior in time series for these measurements varies in non-smoothly form. Therefore if a 16 bit grayscale image is used for these measurements then the low values which their time is very close to the time of the high values will not clearly appear in grayscale image. The reason for this phenomenon is due to the basic colors used in grayscale image which are white, black and other colors in which their intensity degree are between them. So, the pixels which have high darkness intensity reflect their darkness to their neighborhood pixels which have very low darkness intensity. Maybe grayscale image is a good choice for other kinds of measurements which their nature behavior in time series varies in smooth form such as measurements of ambient temperature.

Digital Radiation Image Creation

The processes for creating the digital radiation image are as follows:

- a. Collecting all radiation measurements in one year from radiation monitoring station.
- b. Putting these measurements in a 365×288 array of radiation measurements. The number of rows is equal the number of days in one year and the number of columns equals to the number of measurements in one day which equals to twelve measurements per hour multiplied by 24 hours daily.
- c. Creating another three arrays. The size of each array is the same as the pervious array. The elements of the first array represent the red components, the elements of the second array represent the green components, and the elements of the third array represent the blue components.
- d. Converting each radiation measurement to fuzzy number or linguistic status ^[3] according to allowed limit that is set up by environmental law number four in Egypt ^[4]. This is necessary to establish a meaningful system for creating a digital radiation image. The value for this allowed limit does not exceed 2.3×10^{-7} Sv / hr.

Table 1 shows all fuzzy numbers and their linguistic expressions used in this study.

- e. Determining the color for each radiation measurement by using rule based structure of fuzzy logic ^[5]. The series of fuzzy rules for all measurements were recorded in one year defines the digital radiation image. Defining that Radiation Measurement as RM. These rules are as follows:-

- R₁: IF RM IS UL_ST1 THEN RM_color IS WHITE.
- R₂: IF RM IS UL_ST2 THEN RM_color IS LIGHT BLUE SKY.
- R₃: IF RM IS UL_ST3 THEN RM_color IS BLUE SKY.
- R₄: IF RM IS UL_ST4 THEN RM_color IS LIGHT BLUE.
- R₅: IF RM IS UL_ST5 THEN RM_color IS BLUE.
- R₆: IF RM IS UL_ST6 THEN RM_color IS DARK BLUE.
- R₇: IF RM IS NL_ST1 THEN RM_color IS LIGHT GREEN.
- R₈: IF RM IS NL_ST2 THEN RM_color IS GREEN.
- R₉: IF RM IS NL_ST3 THEN RM_color IS DARK GREEN.
- R₁₀: IF RM IS AL_ST1 THEN RM_color IS VERY DARK GREEN.
- R₁₁: IF RM IS AL_ST2 THEN RM_color IS LIGHT YELLOW.
- R₁₂: IF RM IS AL_ST3 THEN RM_color IS YELLOW.
- R₁₃: IF RM IS AbL_ST1 THEN RM_color IS LIGHT ORANGE.
- R₁₄: IF RM IS AbL_ST2 THEN RM_color IS ORANGE.
- R₁₅: IF RM IS AbL_ST3 THEN RM_color IS BROWN.
- R₁₆: IF RM IS OL_ST1 THEN RM_color IS LIGHT PINK
- R₁₇: IF RM IS OL_ST2 THEN RM_color IS PINK
- R₁₈: IF RM IS OL_ST3 THEN RM_color IS DARK PINK.
- R₁₉: IF RM IS OL_ST4 THEN RM_color IS LIGHT RED.
- R₂₀: IF RM IS VOL THEN RM_color IS RED.
- R₂₁: IF RM IS NO_DATA THEN RM_color IS BLACK.

- f. Putting the value for red component in the first array, green component in the second array and blue Component in the third array according to radiation measurement color produced from step number five. Hence the three images are ready for forming the RGB image which is the digital radiation image.
- g. To make the final image more clear increase its width by repeating each pixel in every

row four times. So, the resulted image dimension is 365×1512 .

Fig. 3a shows how to implement the previous steps for Gamma radiation station located in Cairo city in Egypt. The starting date at one January 2007 from 12:00 am to 1:30 am and the ending date is at three January 2007 from 12:00 am to 1:30 am.

The final image resolution in Fig. 3a is six columns and three rows. Gamma levels measurements with negative values means missed data or unregistered measurement.

Fig. 3b shows the final output result which is Digital Radiation image for Gamma radiation station located in Cairo city in Egypt at 2007. This digital radiation image expresses the all registered and unregistered Gamma radiation measurements at year 2007.

Using image restoration technique for prediction of Gamma radiation levels

Previous section led us to use an image processing technology to integrate the digital radiation image using image restoration technique. The main job from this technique is considering the black points in the digital radiation image as noisy points then covering those points. Our technique for restoration this points is accomplished by dividing the Gamma radiation image into two groups of micro images [6, 7]. All micro images in both groups have the same size. The first group contains all micro images in which these images do not include any missed point. The second group contains small sub-groups of micro images in which any image of them include at least one missed point. Each sub-group contains all micro images which are taken around every one missed point. Fig.4 shows how these processes are performed [8, 9]. The color suggested for the missed point is the color of point of the same location in the same micro image from the first group. The next step is getting the color for every missed point by the color, which has the highest membership function value. The initial membership function of each color is determined by determining the number of all matching points n between each micro image from the sub-group which is from second group to each complete micro image from first group. Then the initial membership function is calculated from the equation (1) [10].

$$\text{Initial Membership} = 10^{-n} \dots \dots \dots (1)$$

Many of initial membership functions for each color are created by repeating the previous step for the reminder of micro images of the sub-group which is from second group. The final membership function for any color is the sum of all initial membership functions that occurred with this color as shown from equation (2)

$$\text{Final Membership} = \sum_{i=1}^{i=k} \text{Initial Membership}_i \quad (2)$$

K is the number of occurrences for one color.

The color for the missed point is the color which has the highest final member ship value [11, 12].

This algorithm is summarized in the following steps:-

- a. Suppose we have a digital radiation image X where image X has some missed points.
- b. Divide image X to a group of micro images Y_i . Where $i = 0, 1, 2, 3$, Number of micro images.
- c. The dimension of any Y_i is (3 col \times 3 row).
- d. All Y_i images do not include any missed point.
- e. For every missed point $N_{(j,K)}$ take a micro images Z_j surrounding it.
- f. Dimension of Z is equal to dimension to Y . For all i , for all j , Compare each point in Z_j with each point in Y_i [8].
- g. If missed point coordinates in Z_j is (u,v) then the color suggested for this point is the color of point coordinate (u,v) in Y_i [9].
- h. IF number of matching points for any Z_j and $Y_i = n$ then color initial member ship function $= 10^{-n}$ [10]. Accumulate all initial member ship values for each color to get final member ship value for this color [11].
- i. The color of the missed point in Z_j is the color, which has the highest member ship function [12, 13].
- j. Repeat those steps for all reminder-missed points.

Fig. 4 shows how to determine micro images for both of missed points and unmissed points.

When there are some 3×3 neighborhoods for desired observation are unavailable this prediction algorithm will start to process all the missed points which their 3×3 neighborhoods for desired observation are available. The output result from this step is decreasing the number of missed points. This means that some of 3×3 neighborhoods for desired observation that were unavailable become available. So all unavailable 3×3 neighborhoods for desired observation can become available by repeating the prediction algorithm several times until the number of unavailable 3×3 neighborhoods is zero.

3. Results and Discussion

This model is implemented for forecasting the Gamma radiation levels measurements in ambient air. Fig. 5a shows a complete digital radiation image; Fig. 5b shows this image after making about 9105 missed pixels which represent about 8.5% of the all pixels in the image via evenly distributed random function and Fig. 5c shows the image resulted after processing the image in Fig. 5b using the restoration technique in this model. The total number of accepted

points with error less than 10 % is 90 % from total missed point. Table 2 classifies the predicted missed pixels in Fig. 5c to three groups. This classification is performed according to prediction quality for each pixel. The first group represents the percentage of the predicted pixels in which their prediction quality is 100% or their error is 0%. The second group represents the percentage of the predicted pixels in which their prediction quality is 90% or their error is 10%. The third group represents the percentage of the predicted pixels in which their prediction quality is less than 90% or their error is more than 10%. The values of the prediction quality in table 2 are computed by getting the percentage error between each predicted value in Fig. 5c and its actual value from Fig. 5a.

This model has a powerful feature in which this model can accomplish its task by only one type of measurements while other prediction models need at least three types of measurements. This means that this model produces accepted results by only one type of measurements and this is verified with measurements of gamma levels in this work. In the other side famous prediction models cannot be operated with one type of measurements. They need at least three types of measurements therefore the output result from this model is the best because other famous models will not produce an accepted output with the same data that is used by our prediction model. This means also that this model does not contradict the theory of modeling by suggesting reaching same accuracy that is resulted from famous models with less information.

This feature makes this model less expensive than other models such as deterministic models and neural network models ^[14- 22]. The deterministic models are mathematical models, physical models and chemical models. Both of deterministic model and neural network models require a large amount of data from different types of measurements. These types of measurements may be not available for the user. In this case, the user must buy the unavailable data to operate his or her model. On the other hand, the user can use only one type of data to operate Long term predication model or Short term predication model.

This feature also saves a lot of money, effort and time because any other model requires money to buy the unavailable data and effort for insuring the quality for this data. These two steps will consume a lot of time. In the other hand this prediction model works with only one kind of data. This means that a lot of money, lot of effort and lot of time are saved by using this predication models.

The major advantage from this model is that this model carries a great useful feature for some

continuous monitoring systems. This continuous monitoring systems watch a unique elements such as Gamma radiation levels (which is covered in this study), earth vibration levels, sea levels. These elements are unique because when using other models such as regression model or neural network model many kinds of data are required to initialize their operation and if these kinds of data are few or not exist as in case of continuous monitoring system for earth vibration levels then this prediction model becomes more suitable model for predicting the unique elements than regression model or neural network model. Table 3 summarizes the pervious comparison between this model and other famous models.

The operations of this model are like the operations of the Artificial Neural Network ANN. The micro images in the first group are considered as a training dataset but this model needs only one training cycle in case of all 3×3 neighborhoods for desired observation are available while ANN needs a lot of training cycles. The micro images in the first group which is described in “Using image restoration technique for prediction of Gamma radiation levels” section contains the necessary training dataset for neighborhoods for desired observation as a predictor and training dataset for non- neighborhoods for desired observation as other predictor.

Since both of this model and ANN model are constructed from training dataset this model has the same problem of ANN model. The performance of this model is affected by the amount of the training data. If the amount of the training dataset is low or the number of missing pixels is high the quality of the performance for this model will be reduced and if the amount of the training dataset is low or the number of missing pixels is low the quality of the performance for this model will be increased. This fact is verified by applying experimentation to the prediction of this model with different ratios of missing pixels. When the ratio of missing pixels is less than or equal 15% the performance of the prediction quality is varying linearly from 95% to 90%. When the ratio of missing pixels is greater than 15% and less than or equal 30% the performance of the prediction is varying linearly from 90% to 83%. When the ratio of missing pixels is greater than 30% and less than or equal 40% the performance of the prediction quality is varying linearly from 83% to 70%. When the ratio of missing pixels is greater than 40% the performance of the prediction quality is not accepted. In other wards the limitation of this model is done when the ratio of missing pixels is greater than 40%.

There is a special problem with this model or another limitation. This limitation is seldom

happened when the frequency distribution for the magnitude of one value in the training dataset is very high. In this case the output from the prediction model also has high frequency distribution for the same value. The good illustration of this limitation is a period between October and November on Fig. 6b. The output data of this period seems to be non-meaningful but the prediction performance is not affected from this limitation because this output reflects the nature behavior of the training dataset which is also the nature behavior of the actual output.

Important information can be obtained in just few minutes by watching the digital radiation image in Fig. 5a such as the value of maximum and minimum measurements in the year and date of them, the most repeated measurement value in the year and the number of times that the radiation station did not work with their date and time. As shown in Fig. 5c the following information can be estimated in few minutes about Gamma radiation measurements in Cairo city in 2007.

Table 1: Fuzzy values for gamma radiation levels.

Fuzzy Number	Linguistic meaning	Fuzzy value
UL_ST1	Under allowed limit stage one	$0 \leq \text{UL_ST1} \leq (0.044 * \text{Allowed limit})$
UL_ST2	Under allowed limit stage two	$\text{UL_ST1} < \text{UL_ST2} \leq (0.087 * \text{Allowed limit})$
UL_ST3	Under allowed limit stage three	$\text{UL_ST2} < \text{UL_ST3} \leq (0.13 * \text{Allowed limit})$
UL_ST4	Under allowed limit stage four	$\text{UL_ST3} < \text{UL_ST4} \leq (0.174 * \text{Allowed limit})$
UL_ST5	Under allowed limit stage five	$\text{UL_ST4} < \text{UL_ST5} \leq (0.217 * \text{Allowed limit})$
UL_ST6	Under allowed limit stage six	$\text{UL_ST5} < \text{UL_ST6} \leq (0.261 * \text{Allowed limit})$
NL_ST1	Near from allowed limit stage one	$\text{UL_ST6} < \text{NL_ST1} \leq (0.304 * \text{Allowed limit})$
NL_ST2	Near from allowed limit stage two	$\text{NL_ST1} < \text{NL_ST2} \leq (0.348 * \text{Allowed limit})$
NL_ST3	Near from allowed limit stage three	$\text{NL_ST2} < \text{NL_ST3} \leq (0.393 * \text{Allowed limit})$
AL_ST1	At allowed limit stage one	$\text{NL_ST3} < \text{AL_ST1} \leq (0.435 * \text{Allowed limit})$
AL_ST2	At allowed limit stage two	$\text{AL_ST1} < \text{AL_ST2} \leq (1.304 * \text{Allowed limit})$
AL_ST3	At allowed limit stage three	$\text{AL_ST2} < \text{AL_ST3} \leq (2.174 * \text{Allowed limit})$
AbL_ST1	Above allowed limit stage one	$\text{AL_ST3} < \text{AbL_ST1} \leq (3.04 * \text{Allowed limit})$
AbL_ST2	Above allowed limit stage two	$\text{AbL_ST1} < \text{AbL_ST2} \leq (3.91 * \text{Allowed limit})$
AbL_ST3	Above allowed limit stage three	$\text{AbL_ST2} < \text{AbL_ST3} \leq (4.34 * \text{Allowed limit})$
OL_ST1	Over allowed limit stage one	$\text{AbL_ST3} < \text{OL_ST1} \leq (13.04 * \text{Allowed limit})$
OL_ST2	Over allowed limit stage two	$\text{OL_ST1} < \text{OL_ST2} \leq (21.73 * \text{Allowed limit})$
OL_ST3	Over allowed limit stage three	$\text{OL_ST2} < \text{OL_ST3} \leq (30.43 * \text{Allowed limit})$
OL_ST4	Over allowed limit stage four	$\text{OL_ST3} < \text{OL_ST4} \leq (34.18 * \text{Allowed limit})$
VOL	Very over allowed limit	$\text{VOL} > \text{OL_ST4}$
NO_DATA	No data recorded at this date	\emptyset

- Maximum measurements value is recorded in the period from 7th March to 15th November from 8:00 am to 10:00 am and their values are AL_ST1 and AL_ST2 in 2007.
- Minimum measurements value is UL_ST2 at various times in the year.
- The most repeated value in year 2007 is UL_ST6.
- The number of days that the station did not work in year 2007 is about seven days, two days in the first week of June, two days in the third week of July and three days in the fourth week of July.

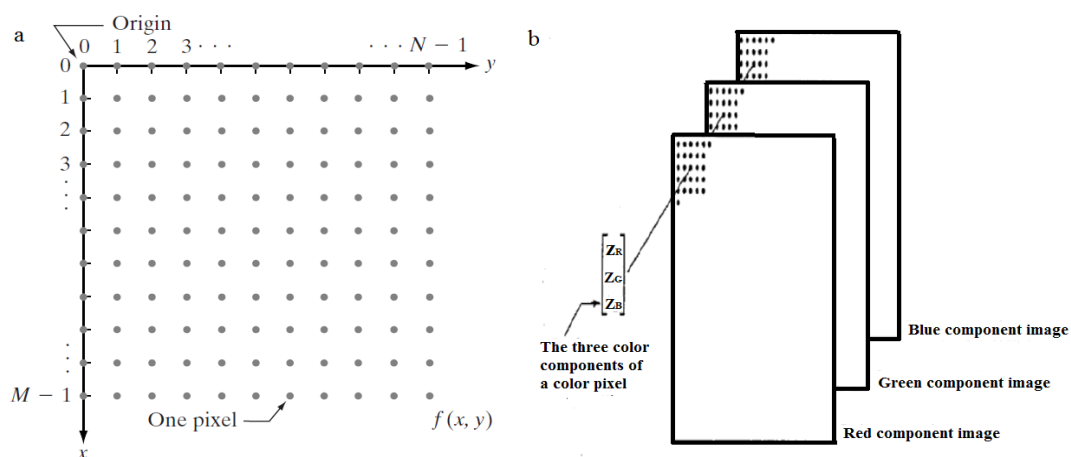
Fig. 6a shows the digital radiation image for Cairo city at 2010. This digital radiation image shows that there are some days do not have any measurements. Fig. 6b shows the same digital radiation image after applying our model. Fig. 5d shows the keys for colors in each image with their fuzzy values.

Table 2: Classifying the predicted pixels according to their predication quality

Groups from predicted pixels	% of The amount of each group to amount of all predicted pixels.
First Group: Predicted pixels that their prediction error is 0%	53%
Second Group : Predicted pixels that their prediction error is less than 10%	37%
Third Group : : Predicted pixels that their prediction error is more than 10%	10%
Average Error	9.5%
Total accepted output	90 %

Table 3: Forecasting using digital image processing and other famous models

	Forecasting gamma radiation levels using Digital image processing	Deterministic models and Neural network models
Input	One kind of measurements	At least three kinds of measurements
Performance	Maximum average error = 9.5% Prediction quality = 90%	With the same dataset that is used with our forecasting using digital image processing both of deterministic models and ANN models will not operate because this dataset is insufficient input to initialize their operations [14- 22].
Cost	Only one kind of measurements	Total price of all unavailable kinds of necessary measurements.
Time	Few minutes for operation time	Time spent for getting and insuring the quality of the unavailable kinds of necessary measurements + Few minutes for operation time = few days
Applications	Continues monitoring systems, market forecast, environmental decision-making, and Continues monitoring systems for unique elements	Continues monitoring systems, market forecast, environmental decision-making

**Figure 1** Presentation of digital image by (a) digital monochrome image, and (b) digital (RGB) color image

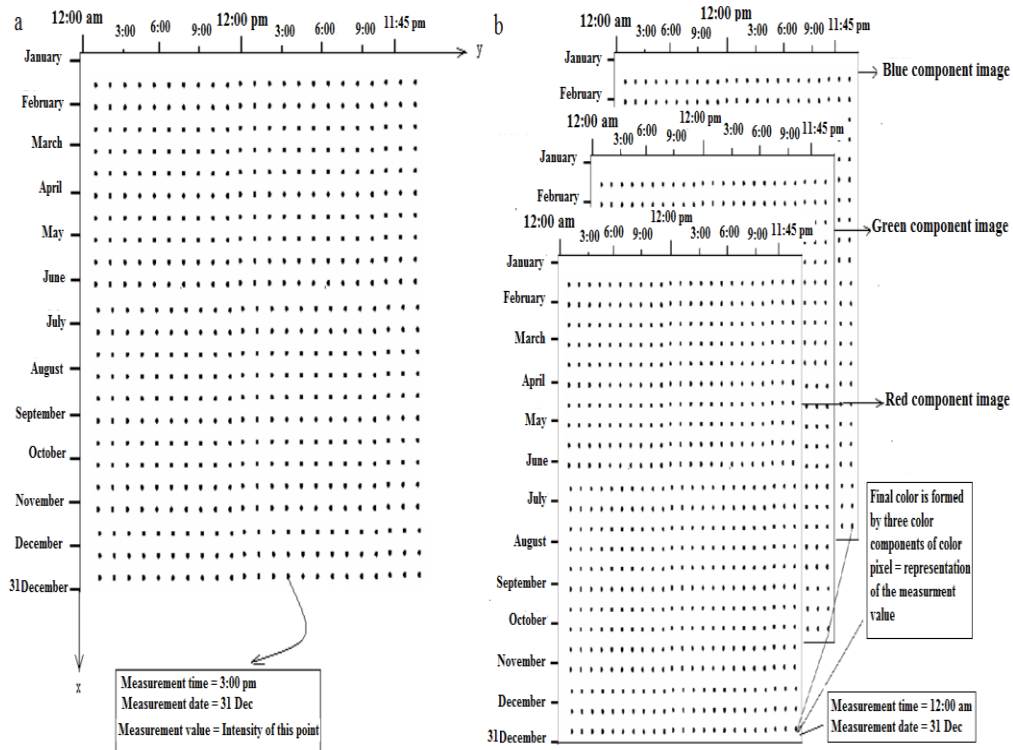


Figure 2 Presentation of digital measurements image by (a) digital monochrome measurements image and, (b) digital (RGB) measurements color image

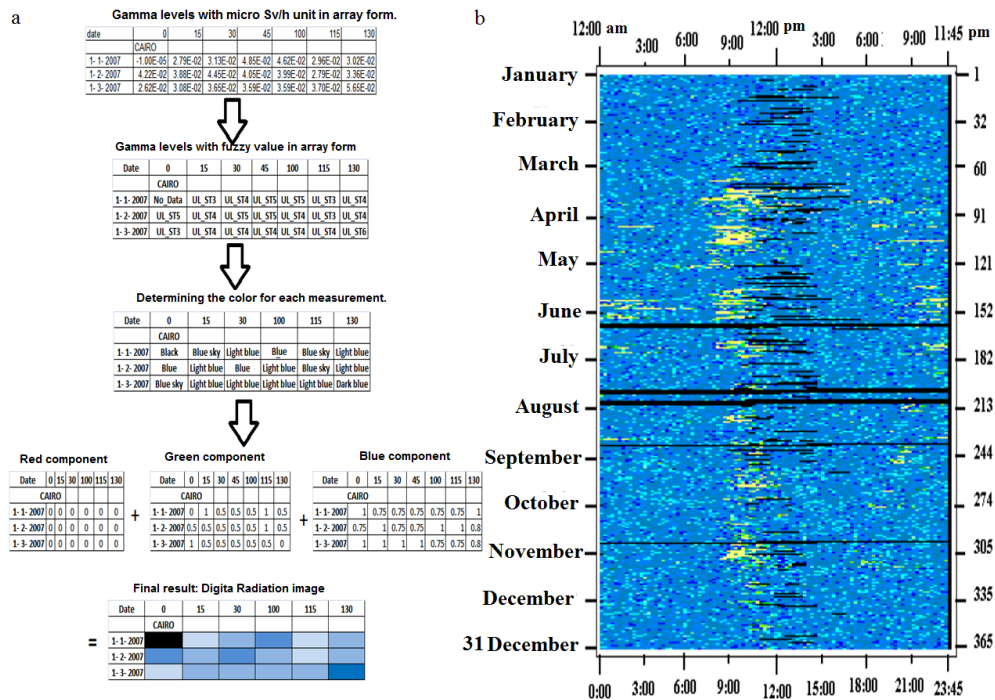


Figure 3 Steps for creating small digital radiation image as shown in (a) and Digital Radiation image for Cairo city for year 2007 as shown in (b)

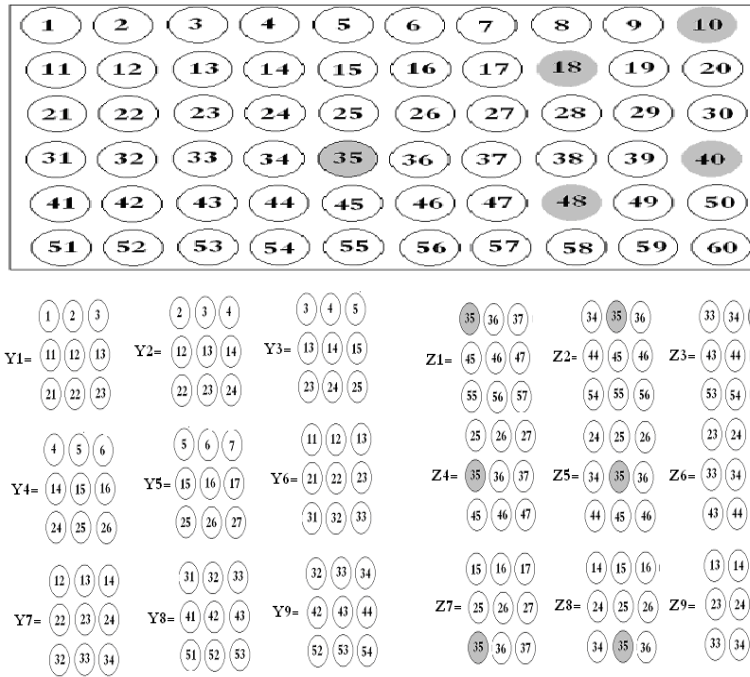


Figure 4 Digital radiation images X which is presented by a rectangle, gray circles are missed points, Y1 to Y9 is micro images and Z1 to Z9 is micro images that are surrounding the point number 35.

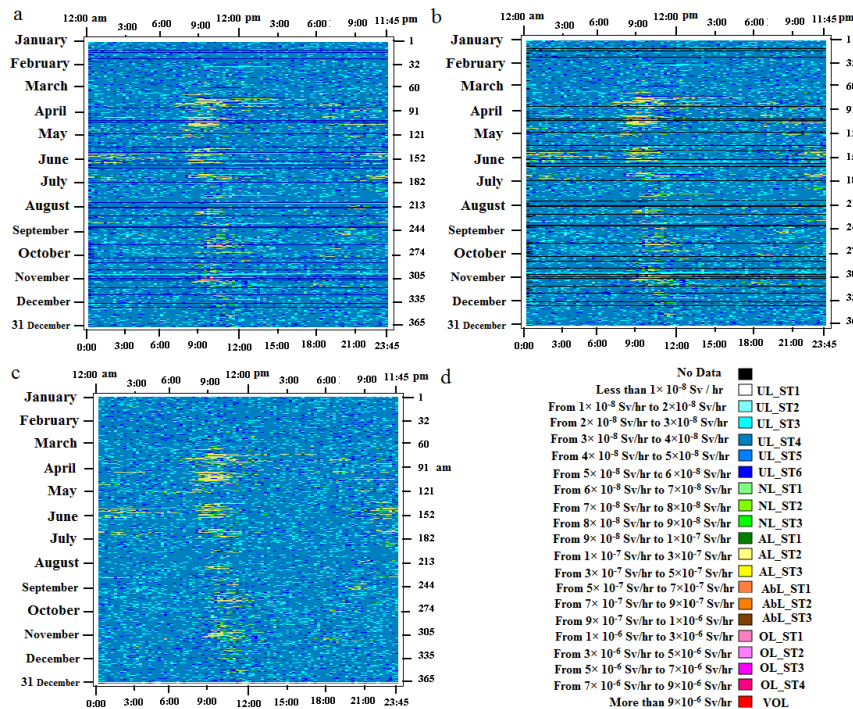


Figure 5 Digital radiation image for Cairo at 2007 without missed points (a), digital radiation image for Cairo at 2007 after making some missed day (b), Image resulted after processing the image in (b) using the restoration technique in this research (c) and color keys for each point in digital radiation image with their fuzzy values (d).

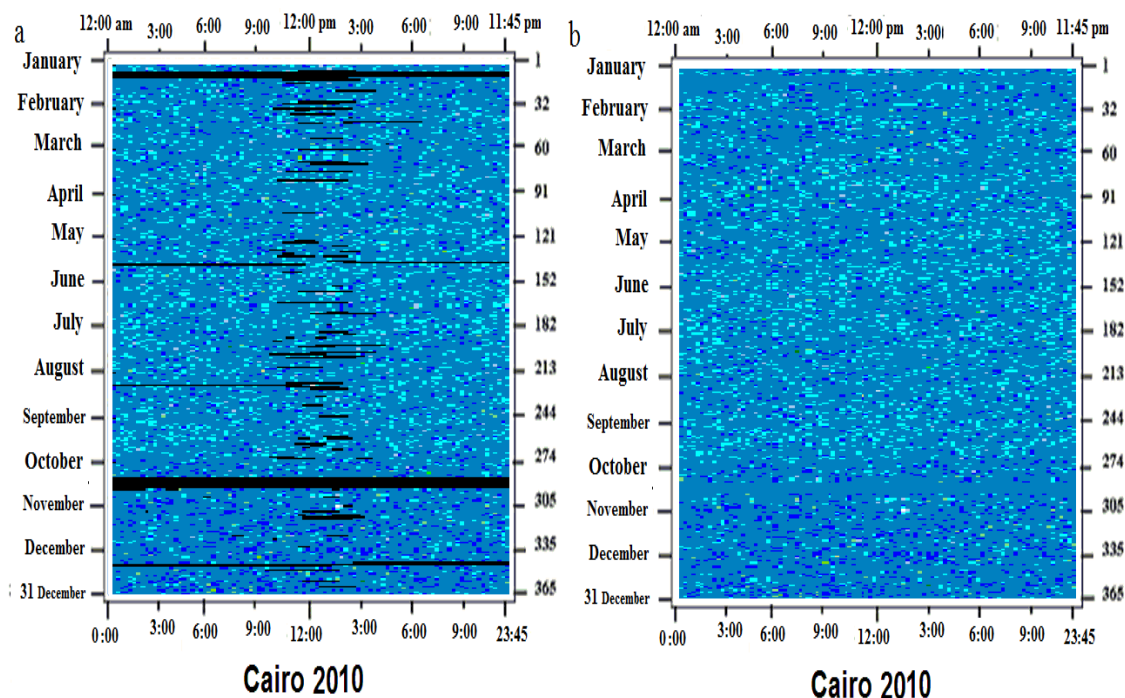


Figure 6 Actual digital radiation image for Cairo at 2010 (a) and digital radiation image for Cairo at 2010 after processing all missed points (b), Image resulted after processing all missed points in image (a) using the restoration technique in this research.

Conclusions

The results from this model are good enough to depend on them for forecasting, recognizing the artificial or strange phenomena, covering lost or missing data and making a temporally monitoring system. This model is better than other famous models when the prediction is only required and only one type of measurements is available because this model is designed to overcome the common limitation with famous prediction models. This common limitation is that the famous prediction models need at least three types of measurements to start their operations.

This model can be used in many applications such as continuous monitoring systems, market forecast and environmental decision-making and this model becomes more suitable model for predicting the unique elements than regression model or neural network model.

Digital Radiation image is more useful tool than other conventional data visualization tools for watching a huge number of measurements which is included in a database of any digital monitoring system. It is a good tool for making a quick analysis for radiation measurements because it has the ability

to include thousands of measurements in a very clear form through only one picture. In the other side, the maximum number of measurements does not exceed 100 for other conventional data visualization methods. This picture helps the user to study and analyze the behavior of these measurements in few minutes instead of spending few hours in reviewing hundreds of charts for the same measurements. Therefore, a huge amount of effort and time is saved by using the digital radiation image.

The novel components in this work which are measurement image and prediction model which is derived from measurement image can be used for other purposes. The measurement image can be used as a visual database for measurements. The main advantage from this database is that the user can perform a quick query without using a computer. Our prediction model can be used to integrate or assist the preparation processes to operate the famous prediction models when there are some missing data in one or more than one type of measurements. The two novel components which are introduced in this work also presented a new field for modeling, data analysis and data mining.

Corresponding author

Mazhar M. Hefnawi
 Department of National Network for Monitoring
 Radioactivity, Atomic Energy Authority of Egypt,
 Cairo, Egypt
mmaazz_2222@yahoo.co.uk

References

- [1] Gonzalez R, Woods R. Digital Image Processing 2nd ed. Prentice Hall, 2002;1: 10–10.
- [2] Eberline Environmental Monitoring System Software Operation Manual. USA, Eeberline, 1990, pp 1-100.
- [3] William S, Buckley J. Fuzzy Expert system and Fuzzy reasoning. Willey Interscience, 2005; 2: 100-20.
- [4] Law number Four -- Environmental law in Arab Republic of Egypt. Egypt government 1995.
- [5] Weinschenk J, Combs W, Marks R. Proc IEEE Int'l Conference on Fuzzy Systems. Missouri, 2003; 5: 43–5.
- [6] Julien M, Michael E, Guillermo S. Sparse Representation for Color Image Restoration. Institute for Mathematics and its Applications (IMA). 2006; 7:120-31.
- [7] Elad M, Aharon M. Image denoising via learned dictionaries and sparse representation. IEEE Computer Vision and Pattern Recognition (CVPR), 2006; 6:200-7.
- [8] Russo L, Gonzalo N, Arlindo L, Pedro M. Approximate String Matching with Compressed Indexes, Algorithms, 2009; 2: 1105-150
- [9] Dmitriy Z, Daniela R, Jacob F, Samuel G. Armato. Predicting Radiological Panel Opinions Using a Panel of Machine Learning Classifiers. Algorithms, 2009; 2:1473-40.
- [10] Marcel T, Tomàs P, Mercè T, Jordi P. Using the Optical Mouse Sensor as a Two-Euro Counterfeit Coin Detector. Sensors, 2009; 9: 7083-13.
- [11] Zhen E, Michelle X. Visualization and Graphics Technical Committee. IEEE, 2008; 3: 55-8.
- [12] Portilla J, Strela V, Wainwright M, Simoncelli E. Image denoising using scale mixtures of gaussians in the wavelet domain. IEEE Transactions on Image Processing, 2004;13(4): 496–12.
- [13] Chiappini L, Cossu R, Lorenzo M. Computer Graphics International. IEEE, 2004; 10(7): 505-7.
- [14] Azzi M, Johnson G, Hyde R, Young R. Prediction of NO₂ and O₂ and O₃ concentrations for NO_x plumes photochemically reacting in urban air. Mathematical and Computational Modelling, 1995; 21(9):39–50.
- [15] Abdul-Wahab S, Bouhamra W, Ettouney H, Sowerby B, Crittenden H. Development of statistical model for prediction of ozone levels in Shuaiba Industrial Area in Kuwait. Environmental Science and Pollution Research (ESPR), 1996; 3(4):195–10.
- [16] Hsu K, Time series analysis of the interdependence among air pollutants. Atmospheric Environment, 1992; 26(4): 491–20.
- [17] Comrie A. Comparing neural networks and regression models for ozone forecasting. Journal of the Air and Waste Management (J. Air & Waste Manage.), 1997; 47: 653–8.
- [18] Boznar M, Lesjak M, Mlakar A. A neural network-based method for short-term predictions of ambient SO₂ concentrations in highly polluted industrial areas of complex terrain. Atmospheric Environment, 1993; 27: 221–9.
- [19] Ruiz-Sua J, Mayora I, Torres J, Ruiz M. Short-term ozone forecasting by artificial neural networks. Advances in Engineering Software, 1995; 23:143–6.
- [20] Elkamel A. Measurement and prediction of ozone levels around a heavily industrialized area: a neural network approach. Advances in Environmental Research, 2001; 5: 47 -12.
- [21] Walle B, Turoff M. Fuzzy relations for the analysis of traders preferences in an information market game. European Journal of Operational Research (EUR J OPER RES), 2009; 195: 905–8.
- [22] Ido E, Eyal E, Alvin E. A Choice Prediction Competition for Market Entry Games: An Introduction. Games, 2010;(1): 117-20.

2/1/2012